Available online at www.sciencedirect.com
ScienceDirect
Journal of Sound and Vibration 300 (2007) 217–240
JOURNAL OF SOUND AND VIBRATION
www.elsevier.com/locate/jsvi

Maximum likelihood estimation of flexural wavenumbers in lightly damped plates

C.R. Halkyard*

Department of Mechanical Engineering, University of Auckland, Private Bag 92019, Auckland, New Zealand

Received 2 February 2005; received in revised form 27 July 2006; accepted 3 August 2006
Available online 19 October 2006

Abstract

This paper describes the use of the maximum likelihood method to estimate the flexural wavenumber characteristics of a vibrating plate from experimental measurements. The motion of the plate is assumed composed of a set of plane propagating waves of unknown wavenumber and amplitude. The problem of determining the wavenumbers and amplitudes that provide the 'best' fit to the measured data is posed as a nonlinear least-squares problem in which the nonlinear and linear variables can be separated. The maximum likelihood method is then used to solve this problem.

The method is demonstrated in simulations of infinite and finite plates, and the effects of nearfields, damping and measurement noise are investigated. Practical implementation issues, including model deficiency, model adequacy and determining convergence are discussed.

The method is then applied to experimental measurements on both a steel plate and a composite (orthotropic) panel, and the results are compared with theoretical predictions. It is shown that the proposed approach can give a good indication of the propagating wavenumber characteristics of lightly damped plates.

1. Introduction

Wave-based methods of vibration analysis can provide valuable insight into the dynamic behaviour of structures, and are particularly applicable at high frequencies. However, such methods tend to rely heavily on accurate estimates of the vibrational wavenumber. While these can be predicted with reasonable accuracy for simple structural elements at low frequencies if the material properties are accurately known, the degree of complexity and/or uncertainty that is present in real structures often renders predictions unreliable, particularly at higher frequencies. Under such circumstances, the estimation of wavenumbers from physical measurements, via spatial signal processing, becomes desirable. The field of spatial signal processing has received considerable attention from researchers in areas such as radar and sonar. However, structural vibration has a number of characteristics, such as the presence of nearfields, dispersion and modal behaviour, which mean that the identification of the vibrational wavenumber in structures poses different problems, and warrants separate investigation.

*Tel.: +64 9 373 7999; fax: +64 9 373 7479.
E-mail address: r.halkyard@auckland.ac.nz.

0022-460X/$ - see front matter © 2006 Elsevier Ltd. All rights reserved.
doi:10.1016/j.jsv.2006.08.019

Nomenclature

A	complex wave amplitude
$\mathbf{I}$	identity matrix
$\mathbf{T}$	transformation matrix (waves → response)
W	plate response in frequency domain
$\underline{\mathbf{W}}$	vector of plate response measurements
$\underline{\tilde{\mathbf{W}}}$	vector of predicted plate responses
e	base of natural logarithm
i	$\sqrt{-1}$
k	wavenumber, wavenumber component
t	time
x, y	Cartesian coordinates

Greek characters

$\mathbf{\Phi}$	vector of wave amplitudes
χ_2	error functional
∇	gradient
ω	angular frequency (rad/s)
μ	step size parameter
κ	error coefficient ($\chi_2/\|\underline{\mathbf{W}}\|^2$)

Subscripts

j, m, r, s	indices
LS	least squares

Superscripts

†	pseudo-inverse of a matrix
$\perp$	orthogonal projection of a matrix
H	Hermitian (conjugate transpose)

The experimental estimation of wavenumbers in structures that effectively function as one-dimensional (1D) waveguides has been described by a number of researchers, and a number of methods have been applied (e.g. Refs. [1–6]). In contrast, wavenumber identification in 2D structures such as plates has received relatively little attention [7,8]. While Prony's method (and related approaches) [1,9–11], the discrete spatial Fourier transform (DFT) (e.g. Ref. [12]) and correlation methods [7,8] are established methods that are applicable to wavenumber identification in 2D structures, they are all susceptible to significant errors, either due to sensitivity to noise or to the inherent limitations in resolution. These errors may be acceptable in some situations, but in others, greater accuracy is required. Under such circumstances, one option is to search for the solutions that best fit the measured data using 'maximum likelihood' estimation. The maximum likelihood method has been applied to problems in many fields, including wavenumber estimation in beams [2]. However, each application has its own specific characteristics and problems. In this paper, the maximum likelihood method presented in Ref. [2] is extended to obtain estimates of the propagating wavenumbers that are present within a vibrating plate. Specifically, this extension introduces the problem of directionality—the possibility of an infinite number of propagation directions, rather than just two—and the consequent incompleteness (or deficiency) of the model.

The following section outlines the principles of maximum likelihood estimation, as applied to estimation of the vibrational wavenumbers in a plate, and some of the issues that arise from its implementation. Simulations are then performed, and these are used to highlight the theoretical capabilities and limitations of the technique. Practical implementation issues, including model refinement and convergence, are discussed. Finally, propagating wavenumbers are estimated from experimental measurements on steel and composite plates, and the results are compared with predictions.

2. 'Maximum likelihood' estimation of plate wavenumbers

This section outlines the use of 'maximum likelihood' estimation for propagating wavenumbers in a plate. A fuller and more general description of 'maximum likelihood' estimation is given in Ref. [2].

Consider a set of n experimental measurements, $W_1,\ldots,W_n$, of vibration on a panel. If the presence of solely plane waves is assumed, these measurements can be approximated as resulting from a set of waves, each having its own complex amplitude A_j, and trace wavenumbers k_{xj}, and k_{yj} in the x- and y-directions,

respectively. This may be written as

$$W_s = W(x_s, y_s) \approx \sum_{j=1}^{N} A_j \, \mathrm{e}^{-\mathrm{i}(k_{xj}x_s + k_{yj}y_s)} \quad \forall \; s = 1, \ldots, n, \tag{1}$$

where k_{xj}, and k_{yj} may be constrained to be purely real, or can be assumed complex, depending on the intended application. Note that the inclusion of complex wavenumbers allows for the presence of both damping and planar nearfields in the model. However, accounting for general planar nearfields greatly increases the number of waves that are required in the model, and therefore only measurement conditions that approximate far-field behaviour are considered in this paper. In that which follows, mathematical models for the plate motion will be specified in terms of the number of plane propagating waves admitted (i.e. the value of N).

Eq. (1) can be rewritten in matrix form as

$$\underline{\mathbf{W}} \approx \mathbf{T}\,\underline{\mathbf{\Phi}} = \underline{\hat{\mathbf{W}}}, \tag{2}$$

where

$$\underline{\mathbf{W}} = \begin{pmatrix} W(x_1, y_1) \\ \vdots \\ W(x_n, y_n) \end{pmatrix}, \quad \underline{\mathbf{\Phi}} = \begin{pmatrix} A_1 \\ \vdots \\ A_N \end{pmatrix}$$

and

$$\mathbf{T} = [T_{sj}] = [\mathrm{e}^{-\mathrm{i}(k_{xj}x_s + k_{yj}y_s)}]. \tag{3}$$

The goal is then to find the trace wavenumbers, k_{xj}, and k_{yj} and wave amplitudes, A_j, that minimise, in some formal way, the difference between the measurements, $\mathbf{W}$, and the prediction given by the model, $\underline{\hat{\mathbf{W}}}$. This difference can be expressed as

$$\underline{\mathbf{W}} - \underline{\hat{\mathbf{W}}} = \underline{\mathbf{W}} - \mathbf{T}\,\underline{\mathbf{\Phi}}. \tag{4}$$

If the wave amplitudes are estimated using a least-squares fit to the measured data then

$$\underline{\mathbf{\Phi}} = \underline{\mathbf{\Phi}}_{\mathrm{LS}} = \mathbf{T}^{\dagger}\,\underline{\mathbf{W}}, \tag{5}$$

where $\mathbf{T}^{\dagger} = (\mathbf{T}^H\mathbf{T})^{-1}\mathbf{T}^H$ is the pseudo-inverse of $\mathbf{T}$ and H denotes the conjugate transpose of a matrix. The difference between the vector of measurements and the prediction given by the model is thus

$$\underline{\mathbf{W}} - \underline{\hat{\mathbf{W}}} = \underline{\mathbf{W}} - \mathbf{T}\underline{\mathbf{\Phi}}_{\mathrm{LS}} = \underline{\mathbf{W}} - \mathbf{T}\mathbf{T}^{\dagger}\,\underline{\mathbf{W}} = (\underline{\mathbf{I}} - \underline{\mathbf{T}}\,\underline{\mathbf{T}}^{\dagger})\,\underline{\mathbf{W}}, \tag{6}$$

where $\mathbf{I}$ is the identity matrix. It can be seen that this form eliminates the (unknown) wave amplitudes from the difference expression, thereby allowing the identification of the wavenumbers to be performed separately from the estimation of the wave amplitudes.

Denoting $\mathbf{P}_{\mathbf{T}} = \mathbf{T}\mathbf{T}^{\dagger}$ and its orthogonal projection

$$\mathbf{P}_{\mathbf{T}}^{\perp} = \mathbf{I} - \mathbf{P}_{\mathbf{T}}, \tag{7}$$

the difference between the vector of measurements and the vector of predicted values can be written as

$$\underline{\mathbf{W}} - \underline{\hat{\mathbf{W}}} = \mathbf{P}_{\mathbf{T}}^{\perp}\,\underline{\mathbf{W}}. \tag{8}$$

Minimising this difference in a least-squares sense therefore requires minimising of the error functional

$$\chi_2(k_{xj}, k_{yj}) = \left\| \mathbf{P}_{\mathbf{T}}^{\perp}\,\underline{\mathbf{W}} \right\|^2, \tag{9}$$

where $\|\|$ denotes the norm of a vector [13]. Clearly this error functional is dependant on the level of vibration, and thus it is not possible to compare the 'goodness of fit' achieved in different applications simply by comparing the values of the minimised error functionals. It is therefore useful to define an error coefficient,

κ, based on the normalised error functional, such that

$$\kappa = \frac{\chi_2(k_{xj}, k_{yj})}{\| \underline{\mathbf{W}} \|^2} = \frac{\left\| \mathbf{P}_{\mathbf{T}}^{\perp} \underline{\mathbf{W}} \right\|^2}{\| \underline{\mathbf{W}} \|^2}. \tag{10}$$

A variety of minimisation techniques can be applied to the error functional. In this case, for simplicity, the method of steepest descent [14] has been used, and in order to iterate to the 'best' combination of wavenumbers using this approach, initial estimates are required. The quality of these initial estimates is important for two reasons. First, the better the initial estimates are, the more quickly the iterations will converge to a solution of acceptable accuracy. Secondly, and more importantly, the nonlinear nature of the problem means that the error surface will have numerous local minima in addition to its global minimum [15]. Insufficiently accurate initial estimates will cause convergence to one of these local minima, rather than to the desired global minimum. It is therefore necessary to start at a point on the error surface from which a continuously descending path can be followed to the global minimum.

There are a variety of techniques that can be used to obtain the initial estimates. These include Prony's method, a 2D spatial discrete Fourier transform, correlation methods, as described in the Introduction, experimental modal analysis and estimates obtained from approximate material properties. In this paper, the initial estimates have been obtained using a correlation method [7], primarily because the method lends itself to graphical representation of the 'goodness of fit' with the measured data. This representation assists both in the selection of initial estimates and in determining the number of wave components to be modelled.

Successful identification of the global minimum of the error surface does not guarantee accurate estimates of the wavenumbers, for a number of reasons. If the model provides a poor description of the vibrational behaviour of the panel (for example, plane propagating waves are assumed when nearfields or non-planar waves are significant, or the number of waves making a significant contribution to the vibration exceeds the number admitted by the model), the location of the global minimum may not accurately reflect the structural characteristics of the plate. Furthermore, the presence of noise in the measurements has the effect of displacing the global minimum from its ideal position. Thus, as would be expected, the accuracy of the estimates obtained is affected by both the validity of the model and the quality of the data used.

3. Simulations

The following simulations are intended to illustrate the performance of the maximum likelihood method in the identification of propagating wavenumbers in plates. The performance of the method is strongly dependant on the match between the model and the true wave field. This presents a problem in practical applications, as, in general, the nature of the true wave field is not known with any degree of accuracy. In each of the following simulations, no prior knowledge of the structure is assumed. The number of waves included in the initial model, and the initial wavenumber estimates used, have been determined though application of the correlation method [7] to the measured data. Model refinement, when necessary, has been performed using knowledge gained from the measured data and the initial model.

3.1. Plane waves in an infinite plate

The simplest application of the technique is the identification of the wavenumbers of plane propagating waves in a lightly damped infinite plate. Fig. 1 shows the contours of the correlation surface in the presence of two propagating plane waves of equal amplitude. Full details of the simulation are given in Table 1.

The waves have been chosen to be sufficiently close in direction that the correlation method cannot accurately identify the individual wavenumbers, because of inadequate resolution. The correlation method identifies a single wavenumber ($k_x = 3$ rad/m, $k_y = 2$ rad/m), however the elongation of the contours in Fig. 1 suggests the presence of more than one wave. A model assuming two propagating plane waves is therefore used in the maximum likelihood estimation, with the real parts of the two initial wavenumber estimates being based on estimates provided by the correlation method. The imaginary parts of the initial estimates are based on a realistic value of the loss factor.

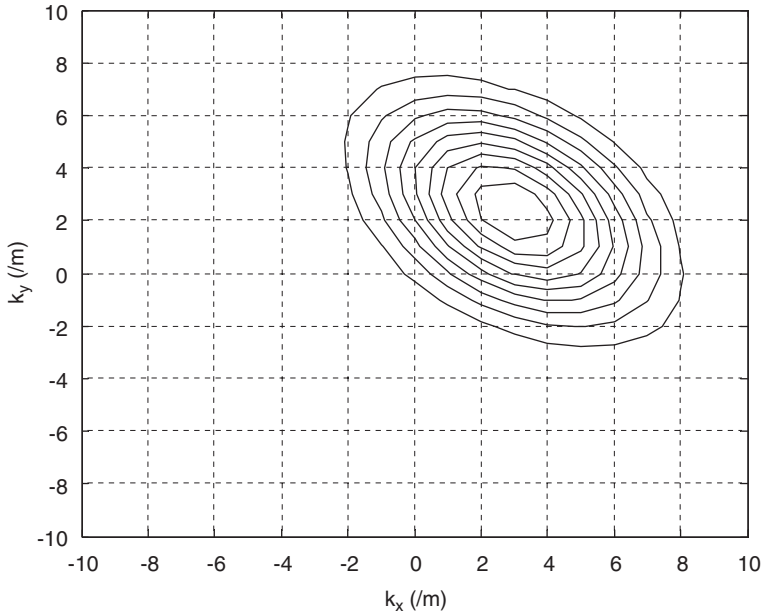

Fig. 1. Correlation contours for wavenumber estimates in 'infinite plate' simulation.

Table 1
Simulation parameters in 'infinite plate' simulations

Amplitude of wave 1 A_1	1
Amplitude of wave 2 A_2	1
Loss factor η	0.01
Trace wavenumbers of wave 1	$k_{1x} = 1.5\pi(1-\mathrm{i}\,\eta/4)$
	$k_{1y} = 0.2\pi(1-\mathrm{i}\,\eta/4)$
Trace wavenumbers of wave 2	$k_{2x} = 0.4\pi(1-\mathrm{i}\,\eta/4)$
	$k_{2y} = 1.3\pi(1-\mathrm{i}\,\eta/4)$
Measurement area	$1\,\mathrm{m} \times 1\,\mathrm{m}$
Number of measurement points	121 (11×11 uniform grid)

The iterations of the maximum likelihood method towards the best wavenumber estimates are shown in Fig. 2. The real and imaginary parts of each of the four trace wavenumber estimates (k_{1x}, k_{1y}, k_{2x}, k_{2y}) are seen to converge to their true values.

The effect of measurement noise on the estimates is seen in Fig. 3. This simulation is identical to the previous one, except that normally distributed random noise is added to the 'measured' data, to give a signal to noise (SNR) ratio of 20 dB. It is apparent that, under these circumstances, the iterations converge to values that are close to the true values, but significant errors have been introduced, particularly in terms of the relative error in the imaginary part of the wavenumber (i.e. the damping component). These errors in the wavenumber estimates give rise to associated errors in the estimated wave amplitudes, which are, in this case ~2–3% in the magnitude, with a phase error of ~0.04 rad. The errors are a consequence of the global minimum of the error surface being displaced from its ideal location by the presence of measurement noise, as described in the previous section. They cannot therefore be addressed through a 'better' search method, as the global minimum is being located correctly. Increasing the dimensions of the measurement array often results in a reduction of this type of error, but in practice the maximum size of the measurement array is usually tightly constrained. Increasing the number of measurement points can also be beneficial if the number of measurements is small, as this effectively results in averaging over a larger number of data

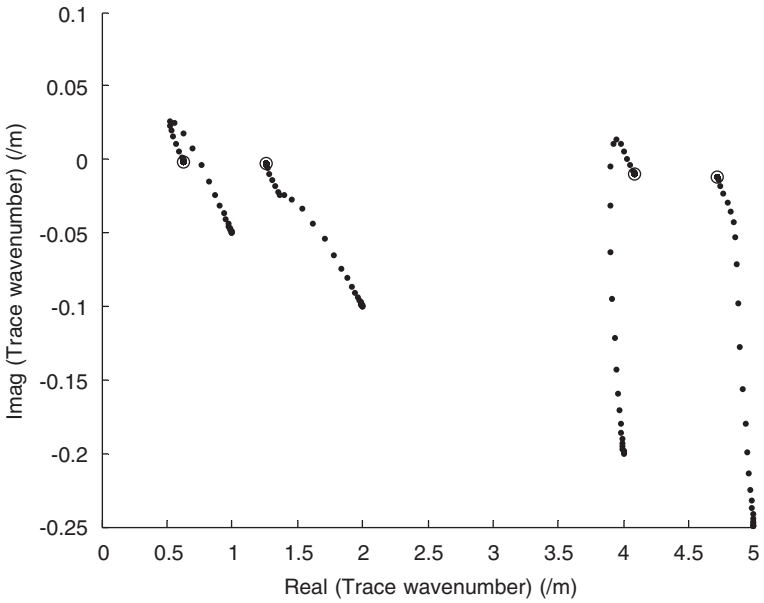

Fig. 2. Convergence of trace wavenumber estimates in 'infinite plate' simulation (ideal data): (●) iterated estimates and (○) true values.

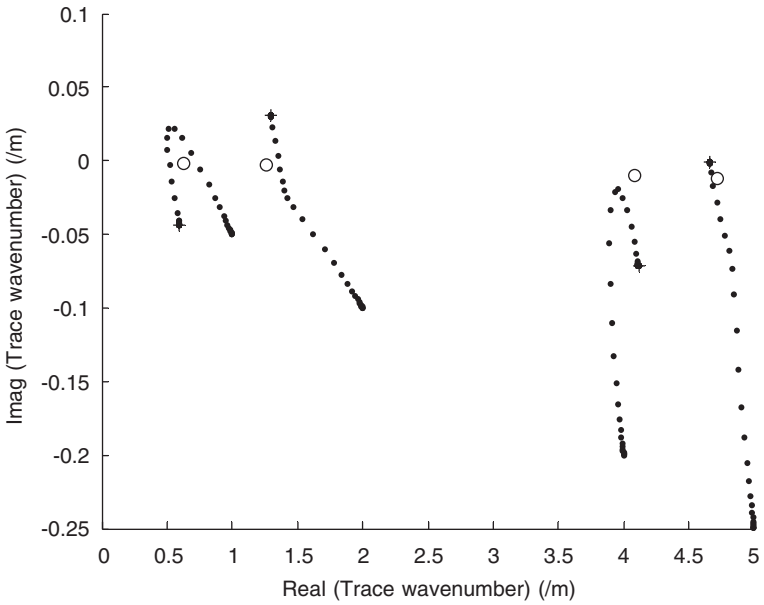

Fig. 3. Convergence of trace wavenumber estimates in 'infinite plate' simulation (SNR = 20 dB): (●) iterated estimates; (+) final estimates; and (○) true values.

points. However, there are practical limits to the number of data points that can be used, and a law of diminishing returns applies.

3.2. Finite plate at resonance

The simplest realistic application for wavenumber identification in two dimensions is the estimation of the wavenumbers present in a lightly damped rectangular plate at resonance. The motion of the plate is then

dominated by a relatively small number of ± propagating plane wave pairs. A relatively simple propagating wave model will therefore give a reasonably accurate description of the wave field, within a region remote from discontinuities, and good performance of the maximum likelihood method would be expected under ideal circumstances. Simulations of this type of structure allow the effects of nearfields and damping on the wavenumber estimates to be investigated.

3.2.1. Simply supported orthotropic plate

Consider a lightly damped (loss factor $\eta = 0.001$), simply supported orthotropic square plate, subject to time-harmonic point excitation at the natural frequency of its (3,3) mode (i.e. the mode shape having three half-trace wavelengths in both the x- and y-directions). This mode has been chosen because of its close proximity to the (4,2) mode, to illustrate the increasing influence of adjacent modes as damping increases. The excitation point is close to the upper right-hand side corner of the plate, to maximise the area in which far-field conditions exist, while the measurement array occupies the left lower quarter of the plate, as shown in Fig. 4, to minimise the influence of the nearfield generated by the excitation. Full parameters for the simulation are given in Table 2.

Application of the correlation method indicates the presence of two dominant propagating wave pairs, as shown by the correlation surface contours in Fig. 5. The locations of the maxima ($k_x = \pm 9.2$ rad/m, $k_y = \pm 9.2$ rad/m) are good estimates of the real parts of the true wavenumbers, which are given by

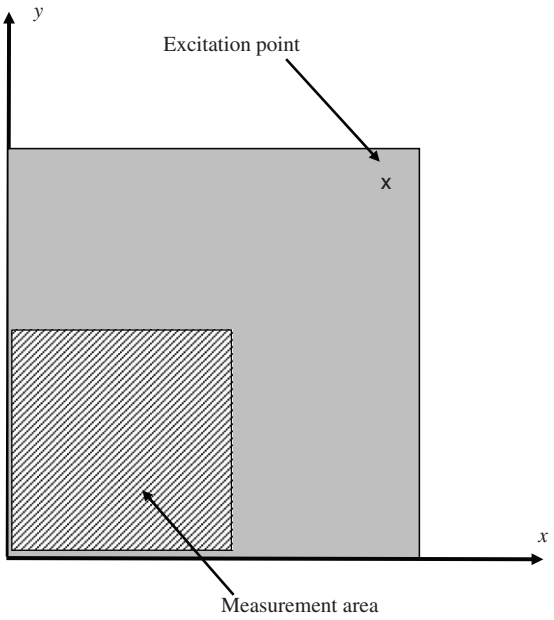

Fig. 4. Plate layout—'simply supported plate' simulations.

Table 2
Simulation parameters in 'simply supported orthotropic plate' simulations

Dimensions of plate	1 m × 1 m
Flexural stiffness ratio	$D_y = 2D_x$, $D_{xy} = \sqrt{D_x D_y}$
Excitation point	$x = 0.975$ m, $y = 0.985$ m
Measurement area	$x = 0$–0.5 m, $y = 0$–0.5 m
Number of measurement points	121 (11 × 11 grid)
Loss factor η	0.001, 0.01, 0.05
Summation over	40,000 modes (0–199 nodal lines in x- and y-directions)

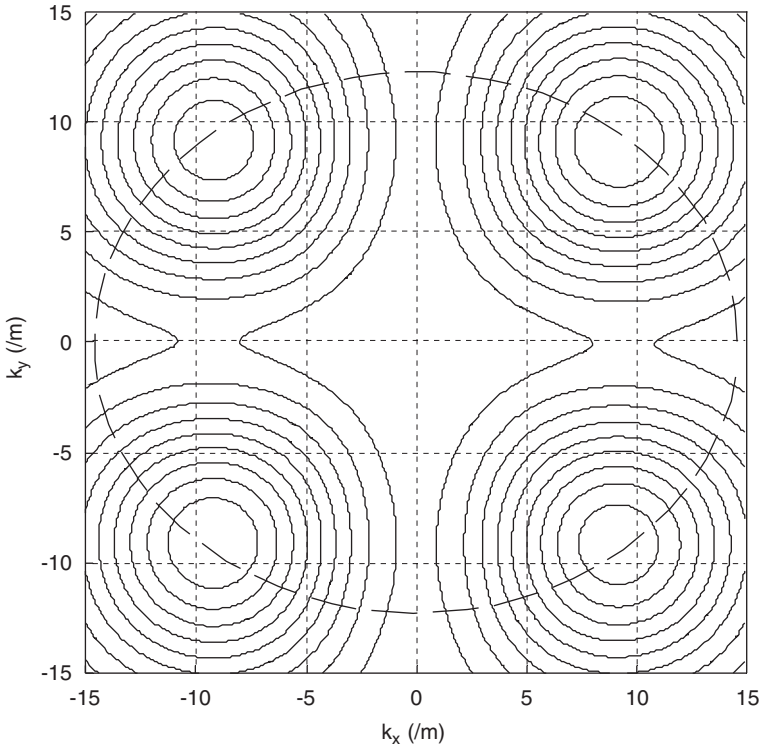

Fig. 5. Simply supported orthotropic plate excited at natural frequency of (3,3) mode ($\eta = 0.001$): (———) correlation contours and (— — —) plate wavenumber.

($k_x = \pm 3\pi$ rad/m, $k_y = \pm 3\pi$ rad/m). However, they can be used as initial values for the maximum likelihood method, using a model that assumes the presence of two $\pm$ propagating wave pairs, i.e.

$$W(x,y) = A_1^+ \, e^{-i(k_{1x}x+k_{1y}y)} + A_1^- \, e^{i(k_{1x}x+k_{1y}y)} + A_2^+ \, e^{-i(k_{2x}x+k_{2y}y)} + A_2^- \, e^{i(k_{2x}x+k_{2y}y)}, \tag{11}$$

to iterate towards a more accurate solution if required, and the results of such an approach are shown in Fig. 6.

The estimation of the imaginary part of the wavenumbers is less satisfactory than that of the real part, owing to deficiencies in the model. Although the motion of the plate is dominated by two (damped) propagating plane waves pairs, there are other, unmodeled, components to the motion. This deficiency has the effect of displacing the global minimum of the error surface from its ideal location, as described in Section 2, leading to errors in the wavenumber estimates. For the case of light damping, the inaccuracy is largely confined to the estimate of the imaginary part of the wavenumber, with the real part being relatively unaffected. This can be explained in terms of the dimensions of the measurement array. Typically, the measurement array will have dimensions of the order of a wavelength or more. The phase change as a wave propagates through the array is therefore significant, and estimates of the real part of the wavenumber that are inferred from this phase change are likely to be reasonably robust. In contrast, if damping is light the effects of damping are small as the wave propagates through the array, and damping estimates inferred from these effects will be very sensitive to noise and model deficiency. Estimates of the imaginary part of the wavenumber are therefore unlikely to be reliable unless there is extremely good agreement between the model and the measured vibration field. This was the case in the 'infinite plate' simulations, and hence the estimates of the imaginary parts of the wavenumbers obtained in these simulations were accurate. However, this agreement between the model and the vibrational field will rarely be achievable in realistic applications. For this reason, subsequent simulations will only concern the estimation of the real part of the wavenumber.

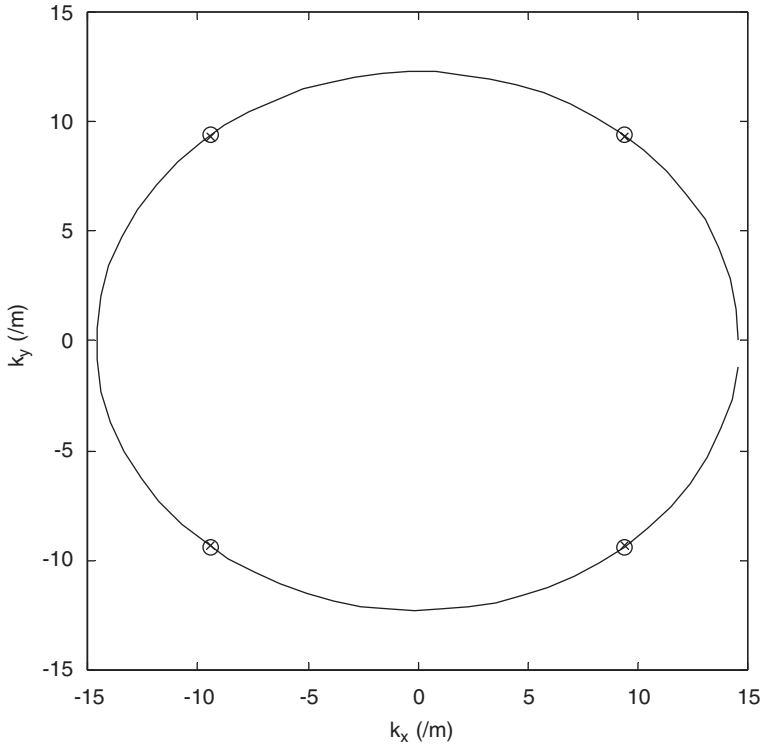

Fig. 6. Wavenumber estimates for simply supported orthotropic plate at natural frequency of (3,3) mode, $\eta = 0.001$, real part: (———) plate theory; (○) theory (3,3) mode; and (×) maximum likelihood estimates.

Increasing the damping in the simulation has three immediate effects. First, an assumption of a purely real wavenumber becomes increasingly inaccurate. Secondly, the assumption of a single mode dominating the response, and the resulting assumption of two dominant propagating wave pairs becomes less valid. This can be expressed in terms of the modal overlap, with a high modal overlap implying that many modes make a significant contribution to the response at a given frequency. The third effect of the increased damping is that the contribution of the direct field becomes more significant relative to the reverberant field. The nearfield associated with the driving point, and the non-planar wavefront of the injected wave, neither of which are included in the proposed model, will therefore have more effect than in the lightly damped case. All of these factors will tend to complicate the estimation of the wavenumber.

The effects of increased damping can be illustrated by a simulation in which the loss factor is increased to $\eta = 0.01$, but all other simulation parameters are left unchanged. Fig. 7 shows the contours of the correlation surface for this simulation, and it is evident that some asymmetry of the contours is present. This indicates the influence of more than one mode of vibration, and therefore suggests that a model representing only two propagating wave pairs may be inadequate. However, the number of significant waves and the approximate values of their wavenumbers are not apparent from Fig. 7. The selection of an appropriate model and initial wavenumber estimates for the maximum likelihood method are therefore not obvious.

One solution to this problem is to apply progressively more complex models and different initial estimates to ensure that the final estimates are insensitive to these changes. If suitable initial estimates cannot be determined by other means (e.g. from the correlation contours), these should be chosen to be of approximately the correct magnitude, and of sufficiently different direction to discourage two or more initial values from converging to the same final estimate. If this occurs, revised initial values should be tried. As patterns emerge in the values estimated by a given model, these should be used as initial values in subsequent models, with the additional initial estimates being chosen to be well-separated from those indicated by the previous model, thereby discouraging multiple components converging to identical, or nearly identical, values. Table 3 shows

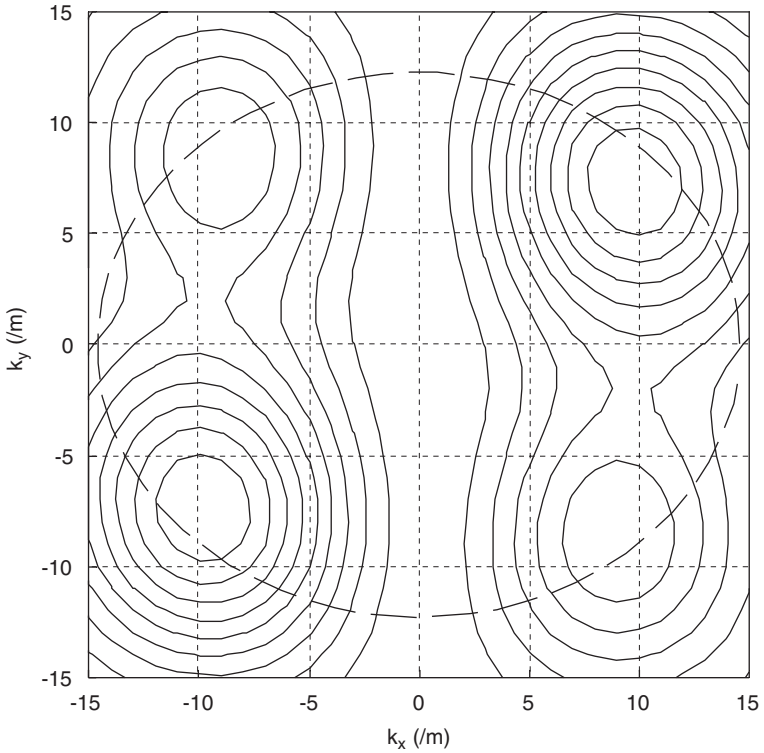

Fig. 7. Simply supported orthotropic plate excited at natural frequency of (3,3) mode ($\eta = 0.01$): (———) correlation contours and (— — —) plate wavenumber.

Table 3
Convergence of wavenumber estimates (rad/m) in simply supported orthotropic plate simulation with increasing model complexity ($\eta = 0.01$)

	4-wave model		8-wave model		12-wave model		16-wave model	
	k_x	k_y	k_x	k_y	k_x	k_y	k_x	k_y
1	10.55	7.48	9.40	9.38	9.43	9.50	9.19	9.51
2	10.50	−8.66	9.28	−9.49	9.49	−9.36	8.94	−9.65
3	−10.50	8.66	−9.60	9.37	−9.62	9.34	−9.48	9.43
4	−10.55	−7.48	−9.38	−9.34	−9.54	−9.36	−9.31	−9.45
5			12.65	6.36	12.56	6.27	12.39	6.79
6			12.60	−6.27	12.65	−6.25	12.71	−6.13
7			−12.64	5.99	−12.64	6.15	−12.53	6.33
8			−12.58	−6.55	−12.59	−6.31	−12.48	−6.54
9					7.22	7.95	2.10	11.78
10					7.23	−10.50	2.10	−10.59
11					−7.02	8.52	−1.95	10.73
12					−6.99	−8.74	−2.11	−11.50
13							13.15	1.69
14							10.68	−8.63
15							−13.01	1.48
16							−9.80	−7.48
Error coefficient κ	0.0505		9×10^{-6}		1.6×10^{-6}		1×10^{-7}	

the wavenumber estimates obtained using the maximum likelihood based on models representing four, eight, 12 and 16 propagating waves (i.e. one, two, three and four contributing modes), together with the error coefficient, κ, for each model. It can be seen that the four- and eight-wave model give significantly different estimates of the wavenumbers of the four dominant waves in the plate, indicating that the four-wave model is not adequate in this case. This is further evidenced by the error coefficient, which is substantially smaller (i.e. better) for the eight-wave model than for the four-wave model. In contrast, the eight-, 12- and 16-wave models are in relatively good agreement on the eight dominant wavenumbers in the plate, suggesting that the eight-wave model is the minimum required for wavenumber estimation in this particular application. Further evidence of this is provided by the error coefficients, which are small for all of these models. The adequacy of the eight-wave model is confirmed by Fig. 8, which shows the theoretical plate wavenumbers at this frequency, together with the predictions obtained using the maximum likelihood method. The validity of the remaining four wavenumber estimates provided by the 12-wave model could be assessed by comparison with the 16-wave model. However, increasing the model complexity in this way is computationally expensive, and therefore alternative ways of assessing the validity and importance of these estimates are desirable. The importance, if not the accuracy, of these 'residual' wavenumbers can be estimated by estimating the amplitudes of the associated waves through wave decomposition. In this case, the amplitudes of these four residual waves are small (of the order of a few percent) relative to the eight dominant waves. Increasing the number of propagating waves in the model beyond 12 is therefore unlikely to improve the estimates of the eight dominant wavenumbers significantly. Furthermore, the sensitivity of the four 'residual' wavenumber estimates to the initial values suggests that they are merely an artefact of the minimisation behaviour, rather than truly reflecting the propagation characteristics of the plate. If this is the case, further model refinement through the incorporation of more plane propagating waves will be ineffective. The validity of these inferences is confirmed by comparison with the 16-wave model, which gives markedly different estimates for the 'residual' wavenumbers, indicating that 'converged' estimates have not yet been reached.

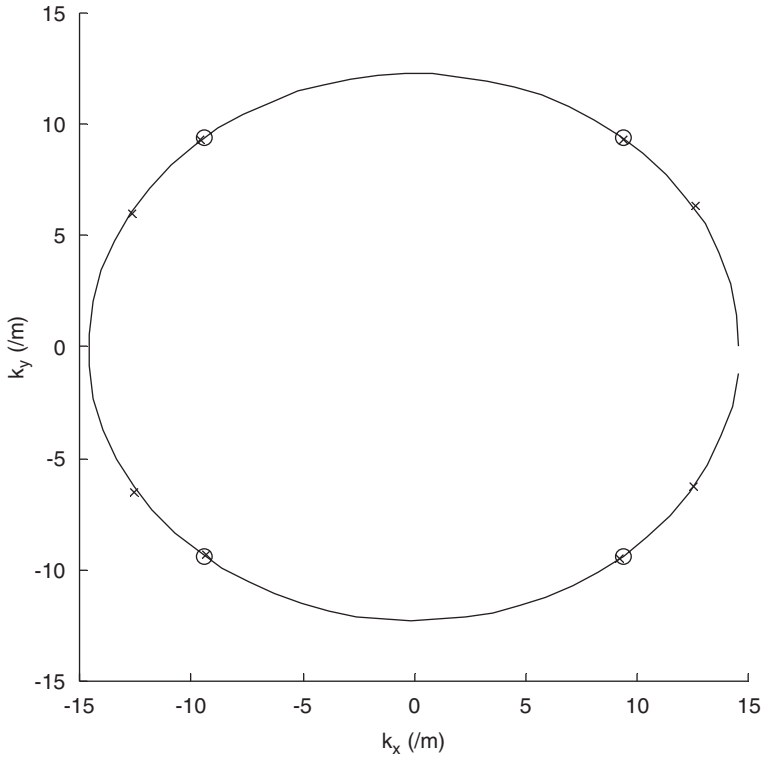

Fig. 8. Wavenumber estimates for simply supported orthotropic plate excited at natural frequency of (3,3) mode, $\eta = 0.01$, real part: (———) plate theory; (○) theory (3,3) mode; and (×) maximum likelihood estimates (eight-wave model).

3.2.2. Free isotropic plate at resonance

The previous simulation of a simply supported plate avoided the need to consider the presence of nearfields at the plate boundary. In contrast, the following simulation of a lightly damped, free square isotropic plate introduces nearfields at the boundaries of the plate. The motion of the plate in its fourth mode is simulated [16], and thus the nearfield and the non-planar wavefront associated with point excitation are avoided. This allows the effects of the boundary nearfields to be isolated from other sources of error.

In the first simulation, it is assumed that the measurement array (441 points in a uniformly spaced square grid) covers the entire plate. The outer sensors of the array are therefore strongly influenced by the nearfields that are present close to the plate boundary. Fig. 9 shows the correlation contour obtained from these measurements. The symmetry suggests that the motion is dominated by two $\pm$ propagating wave pairs, with wavenumbers ($k_x \approx \pm 3.3$, $k_y \approx \pm 3.3$). Using these as initial values for the maximum likelihood method, in conjunction with a model that assumes the existence of two $\pm$ propagating wave pairs, provides a better estimate of the plate wavenumber. The results of this simulation are shown in Fig. 10. It can be seen that the maximum likelihood method improves the estimate of the plate wavenumber, but there is still a significant discrepancy between the final iterations and the theoretical values. This discrepancy is a consequence of the nearfields at the boundaries of the plate, which are ignored in the model.

The effect of the nearfields on the wavenumber estimate can be reduced by reducing the size of the measurement array, so that the outer sensors are somewhat removed from the plate edge and therefore less influenced by the boundary nearfields. However, the reduction in array dimensions is accompanied by a reduction in resolution. This is apparent in the second simulation, in which the sensor spacing is unchanged, but the dimensions of the measurement array are halved while the array remains centred on the centre of the plate. Instead of indicating the presence of four waves (two $\pm$ propagating wave pairs), the correlation surface now has a single maximum at $k_x = k_y = 0$, as seen in Fig. 11, owing to the reduced resolution. Despite this, good estimates of the plate wavenumber can be obtained using the maximum likelihood method and appropriate starting values, as shown in Fig. 12. The improved accuracy given by this reduced array, under

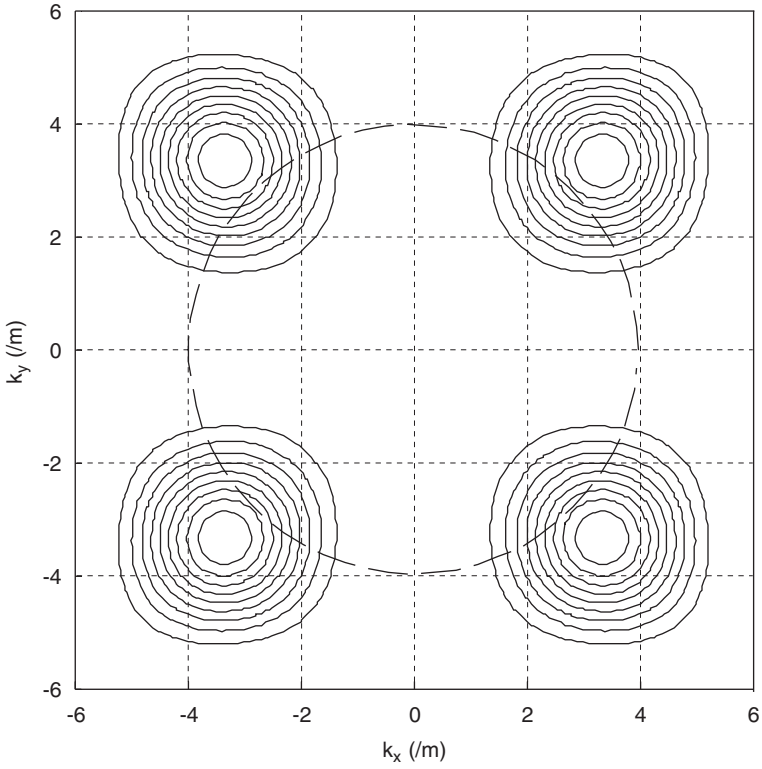

Fig. 9. Free isotropic plate vibrating in fourth mode (full array): (———) correlation contour and (— — —) plate wavenumber (theory).

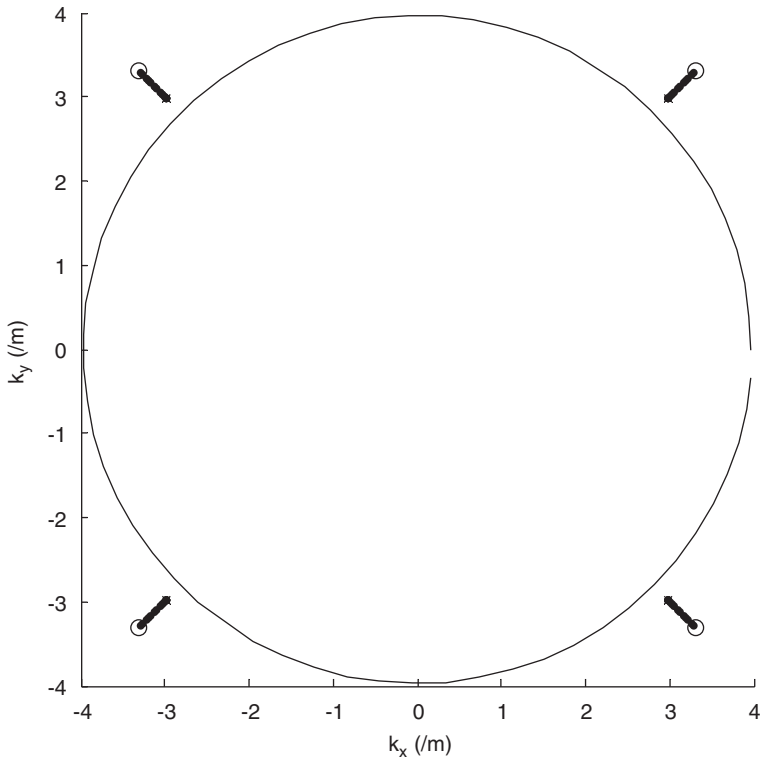

Fig. 10. Convergence of wavenumber estimates in free plate simulation (full array): (———) theory; (○) initial values; (●) iterated estimates; and (×) final estimates.

ideal conditions, is readily apparent when compared with Fig. 10. It should be noted, however, that this improvement comes at a cost of lost resolution and increased sensitivity to noise, and these could have implications on the processing of real data that are not apparent in simulations.

3.3. Non-resonant simply supported plate

The previous simulations have, either explicitly or implicitly, involved vibrational fields that are dominated by a relatively small number of waves. In the following simulation, the non-resonant response of a simply supported orthotropic plate, subject to time-harmonic point excitation, is considered. In comparison to the resonant plate, a larger number of waves make a significant contribution to the response. Consequently, a more complex mathematical model, admitting a larger number of waves, is likely to be necessary. This presents both a problem and an opportunity. The problem lies in the selection of an appropriate model, and in the increased computational requirements. The opportunity is that a larger number of wavenumber estimates can potentially be found at each frequency, giving improved wavenumber-direction information in non-isotropic plates. Again, the required level of model complexity will not generally be known, and must be inferred from agreement between models.

Typically, the non-resonant response will be dominated by those modes having natural frequencies that are ‘close’ to the excitation frequency. Associated with each of these modes is a set of wavenumbers that can be estimated by applying the maximum likelihood method as described in the previous sections, or by using another appropriate estimation technique. These resonant estimates can then be used as initial values when applying the maximum likelihood method to the non-resonant data, and a strategy of increasing model complexity should reveal convergence to consistent estimates for some subset of the wavenumbers once an adequate model is adopted. In this case, model refinement by progressive inclusion of the plane wave sets associated with the ‘next closest’ natural frequency is implemented.

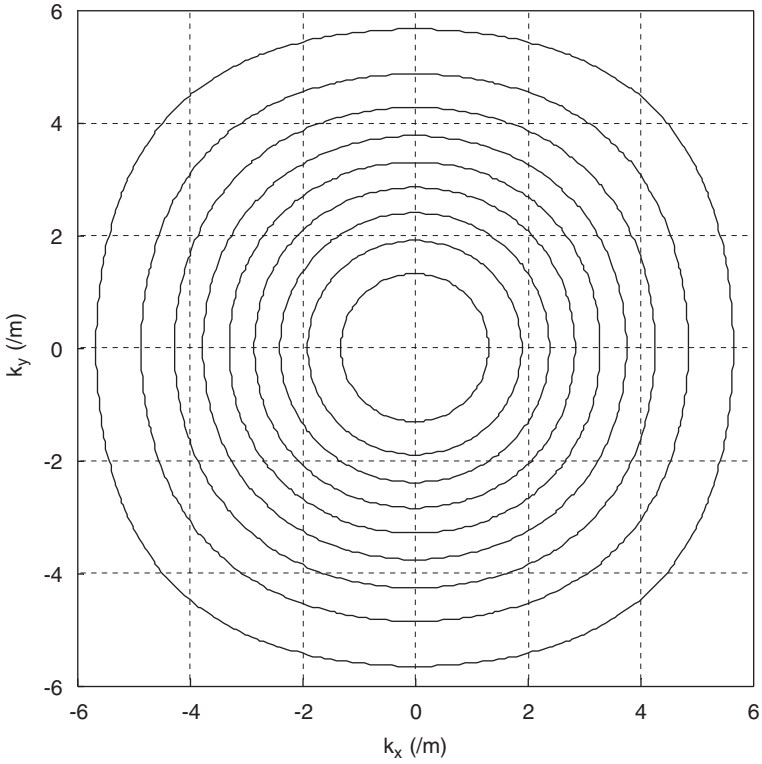

Fig. 11. Free isotropic plate vibrating in fourth mode (reduced array): (———) correlation contour.

The simply supported orthotropic plate is the same as used in earlier simulations, with a loss factor of $\eta = 0.001$. Four adjacent natural frequencies have been identified, and their associated wavenumbers have been estimated as described in the previous simulations.

It is assumed that, at a frequency close to the middle of this range, the response of the plate can be expressed as the sum of the contributions of some or all of these modes, each of which can be expressed as the sum of four propagating plane waves. The wavenumber estimates at the natural frequencies have been used as initial estimates when applying the maximum likelihood method to identify the wavenumbers present at the specified frequency. The wavenumbers have been identified, together with the associated error coefficients, using eight-, 12- and 16-wave (effectively two, three and four significant modal contribution) models. While increasing the order of the model decreased the error coefficient (as would be expected), all models resulted in a relatively small error coefficient κ, and therefore provided a reasonable approximation to the measured data. As a consequence there was relatively good agreement between the models in terms of the estimated wavenumbers. This can be seen in Figs. 13–15, which show the estimated wavenumbers for the three models, together with the predicted plate wavenumbers at that frequency and ellipses fitted, in least-squares sense, to the wavenumber estimates. (Note that the specific form of orthotropy used in the simulations results in an elliptical wavenumber-direction characteristic. This is not the case for general orthotropy.) All models provide a close approximation of the plate wavenumber characteristics.

If the expected form of the wavenumber-direction characteristic is known, fitting of the wavenumber estimates to an appropriate curve, as in the previous graphs, can provide an additional guide to the validity of the wavenumber estimates. Convergence to good estimates can then be judged on the way in which the curve of best-fit changes as the model is refined, and how the individual estimates are scattered about the curve.

At higher levels of damping, it is to be expected that more modes of vibration contribute significantly to the response. It is therefore likely that higher order models will be necessary to obtain reliable

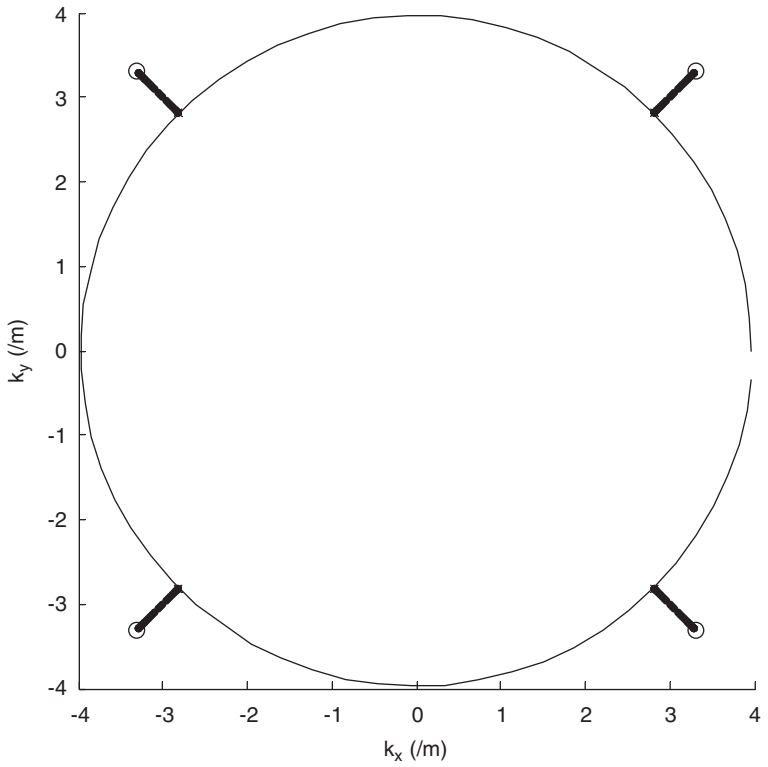

Fig. 12. Convergence of wavenumber estimates in free plate simulation (reduced array): (———) theory; (○) initial values; (●) iterated estimates; and (×) final estimates.

wavenumber estimates. Evidence of this is provided by estimations of the wavenumbers in a plate in which the loss factor is $\eta = 0.05$, but is otherwise identical to the previous simulation. The associated error coefficients are given by $\kappa = 2 \times 10^{-3}$, 1×10^{-5} and 1.2×10^{-6} for the eight-, 12- and 16-wave model, respectively. It is apparent that the error coefficient for the eight-wave model is substantially greater than for the other two models, implying a substantially poorer fit to the measured data. The wavenumber estimates associated with this model are therefore likely to exhibit significant errors. This is confirmed by Figs. 16–18, which show the estimated wavenumbers, together with the theoretical wavenumber-direction characteristics and the 'best fit' ellipses for the three models. It would appear that both the 12- and the 16-wave models provide a good estimate of the plate wavenumber characteristics, as the ellipses that best fit the data are very similar. In contrast, the 'best fit' ellipse of the eight-wave model is significantly different from those of the other two models, indicating that these estimates are unlikely to be accurate. Inspection of the deviation of the individual estimates from the line of best fit suggests that the 12-wave model is the most appropriate in this case. These inferences are confirmed by comparison of the 'best fit' ellipses with the theoretical predictions. Note that the deviation could be more rigorously assessed in terms of the mean squared error, but this has not been attempted.

The effect of measurement noise on the estimates is shown in Fig. 19. The simulation is identical to that in Fig. 17 (i.e. 12-wave model, $\eta = 0.05$), except that normally distributed random noise has been added to the 'measurement' to give a SNR of 20 dB. While the fit with theoretical predictions still appears reasonable, the error coefficients suggest a need for caution. The eight-, 12- and 16-wave models all resulted in error coefficients of $\kappa \sim 0.5 - 1 \times 10^{-2}$, indicating a significant discrepancy between the model predictions and the measured data which did not improve greatly with increasing model order.

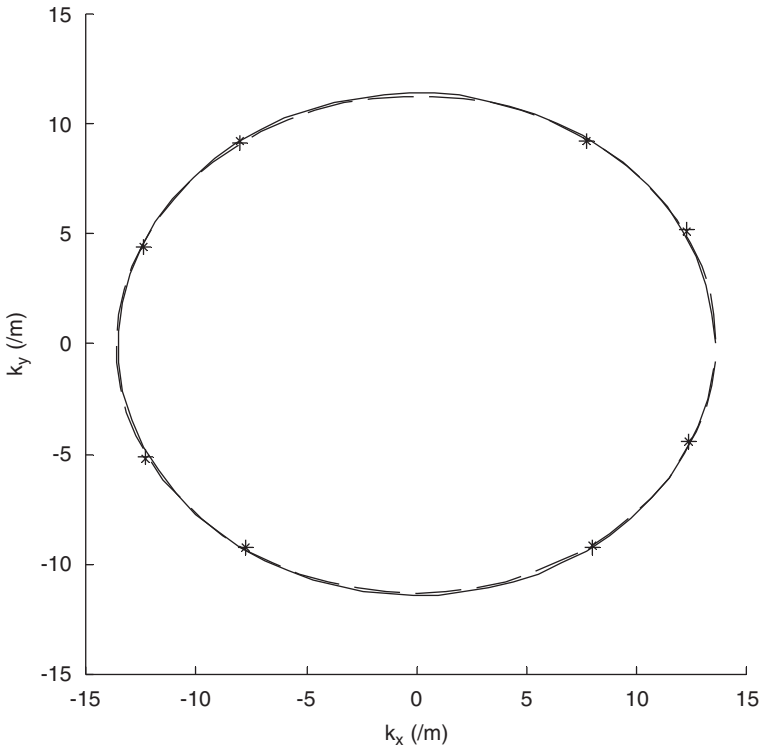

Fig. 13. Wavenumber estimates in non-resonant plate simulation (eight-wave model, $\eta = 0.001$): (———) theory; (+, ×) final estimates; and (— — —) 'best fit' ellipse.

4. Experimental implementation

4.1. Steel plate

A $915 \times 590 \times 1.6$ mm steel plate was suspended by string from two corners, to lie in the vertical plane with the long sides being vertical and the short sides horizontal. The plate was subjected to point excitation, close to its upper right-hand corner, via a Ling V201 electrodynamic shaker, stinger rod and Bruel and Kjaer 8001 force transducer. The response of the plate was measured at 225 points over a 500×500 mm uniform grid, using a Polytec PSV-200 scanning laser vibrometer, and the mobility of each point was calculated.

The wavenumbers at four adjacent natural frequencies were estimated, initially using the correlation method and then refined using the maximum likelihood method. The wavenumbers present at a (non-resonant) frequency in the middle of this band (206 Hz) were then estimated using the maximum likelihood method and progressively refined models, with the wavenumber estimates at the natural frequencies used as initial estimates. (Note: Where this has led to two or more estimates converging to the same value, the initial estimates have been revised.) The estimates obtained, using six- and 10-wave models are shown in Figs. 20 and 21, respectively. The associated error coefficients are relatively large, being $\kappa = 0.075$ and 0.012 for the two models. However, it is apparent from the graphs that, in general, the estimates of the dominant wavenumbers are not changed significantly by increasing the number of waves represented in the model. The more refined model simply provides estimates of a greater number of wavenumbers. This is a good indication that both the models are valid for this application, and that the estimates are reliable. Comparison of the estimates with predictions based on Kirchoff plate theory confirms this observation, with all estimates lying close to the predicted curve, despite the relatively large error coefficients.

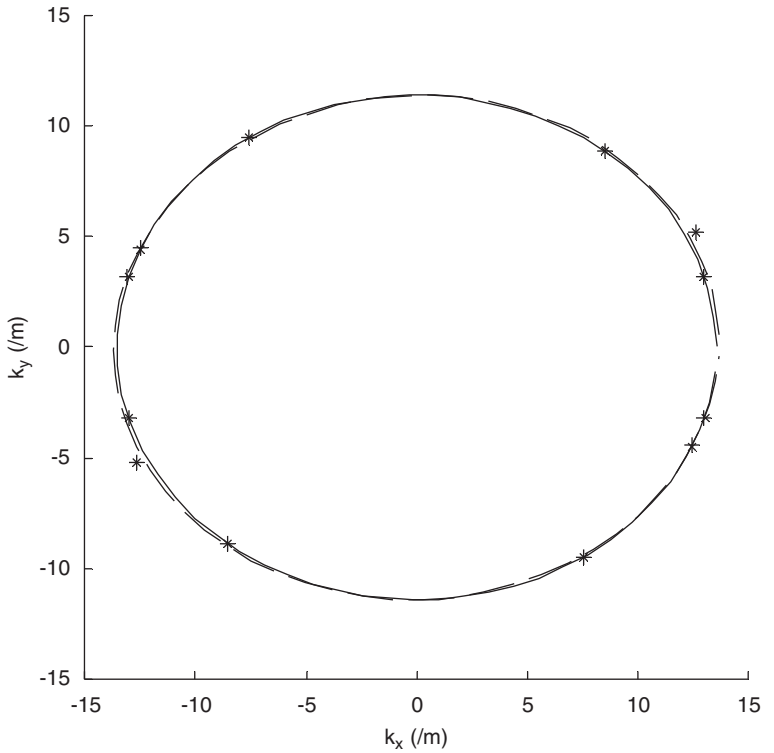

Fig. 14. Wavenumber estimates in non-resonant plate simulation (12-wave model, $\eta = 0.001$): (———) theory; (+, ×) final estimates; and (— — —) 'best fit' ellipse.

4.2. Orthotropic panel

A $960 \times 805 \times 10$ mm flat composite sandwich panel (CFRP skins of $+45/-45/-45/+45$ either side of a ROHACELL-110 foam core) was suspended by string from two corners, to lie in the vertical plane with the long sides being vertical and the short sides horizontal. The plate was subjected to point excitation, close to its upper right-hand corner, via a Ling V201 electrodynamic shaker, stinger rod and Bruel and Kjaer 8001 force transducer. The response of the plate was measured at 225 points over a 700×700 mm uniform grid, using a Polytec PSV-200 scanning laser vibrometer, and the mobility of each point was calculated.

The wavenumbers at five adjacent natural frequencies were estimated, initially using the correlation method and then refined using the maximum likelihood method. The wavenumbers present at a (non-resonant) frequency in the middle of this band (302 Hz) were then estimated using the maximum likelihood method and progressively refined models. The wavenumber estimates obtained, together with the predicted wavenumber characteristics (by Heron [17]) for the orthotropic panel, are shown in Figs. 22–24. The associated error coefficients are $\kappa = 0.009$, 0.004 and 0.0025, respectively. It is apparent from the graphs that the estimates provided by the eight-, 12- and 16-wave models are consistent in terms of their magnitude-direction characteristics, while the error coefficients indicate that model refinement provides a modest improvement in data fitting. Furthermore, the similarity of the individual results obtained from the 12- and 16-wave models give a level of confidence that convergence is occurring, although further verification could be sought, as the evidence is not conclusive. The agreement between the estimates and the predictions indicates that the estimation technique can be used to experimentally determine the wavenumber-direction characteristics of a lightly damped orthotropic panel.

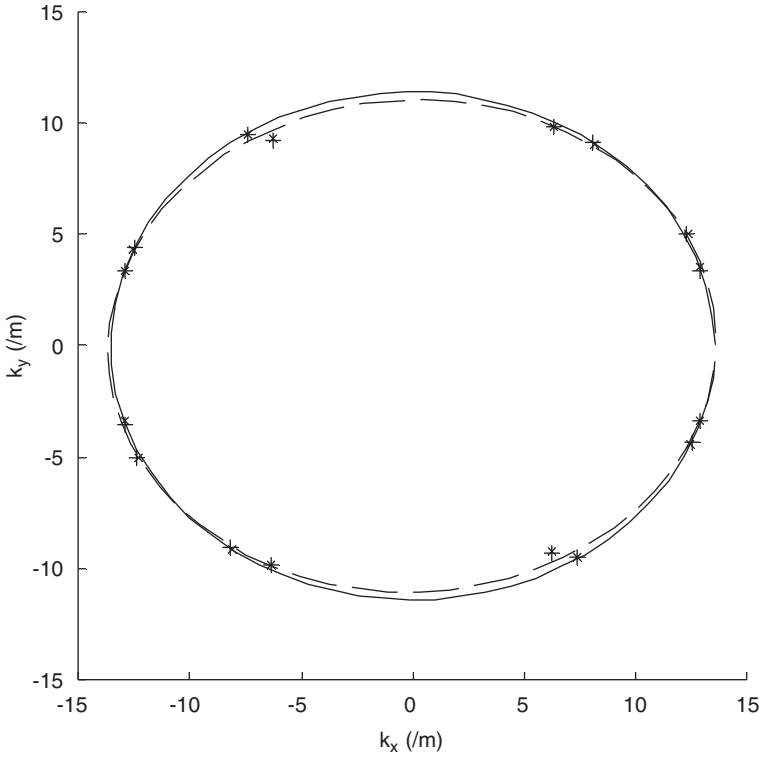

Fig. 15. Wavenumber estimates in non-resonant plate simulation (16-wave model, $\eta = 0.001$): (———) theory; (+, ×) final estimates; and (— — —) 'best fit' ellipse.

5. Conclusions

A technique, based on the maximum likelihood method, for estimating the wavenumbers and amplitudes of plane propagating waves in a plate has been presented. The expected behaviour of the technique has been described, and simulations have been performed to verify this behaviour. Assessment of the adequacy of the model and the accuracy of the results though progressive model refinement has been discussed. The technique has been implemented experimentally, and the results compared with predictions.

It has been shown that the accuracy of the wavenumber estimates is strongly dependant on the model used. If the form of the model accurately reflects the nature of the vibrational field in the measurement region, good estimates can be obtained. However, even small differences between the assumed and true behaviour have a significant effect on the wavenumber estimates. Most strongly affected are the wavenumbers whose wave amplitudes are relatively small, wavenumber component that are small (e.g. the imaginary part, representing damping), and closely spaced wavenumbers. This means that reasonably robust and accurate estimates of the real (propagating) part of the wavenumber can be obtained when the vibration is dominated by a relatively small number of (approximately) plane waves, provided an adequate model is used. Even under these favourable circumstances, however, estimates of the wavenumbers associated with the minor waves are likely to be significantly biased due to model deficiency, and estimates of the imaginary (attenuating) part of the wavenumber are unreliable. The technique is therefore applicable to determining the real (propagating) part of the wavenumber in plates in which the modal overlap is relatively low. Suitable techniques or models for plates with high modal overlap are an area for further study.

The need for an appropriate model of vibrational behaviour of an unknown structure means that practical implementation of the method will inevitably require the application of engineering judgement, and iteration towards valid results. In this way, it has much in common with experimental modal analysis or finite-element

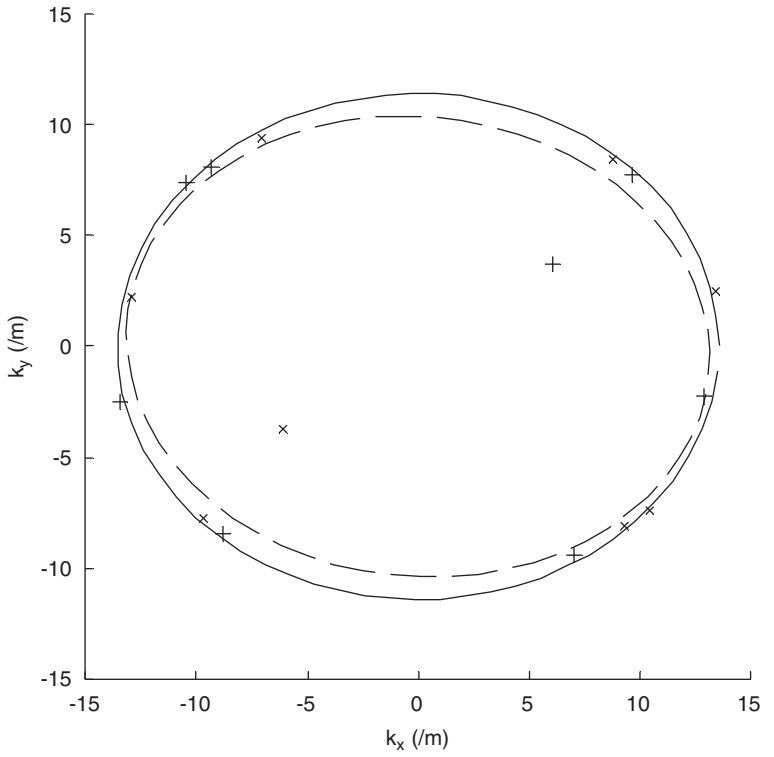

Fig. 16. Wavenumber estimates in non-resonant plate simulation (eight-wave model, $\eta = 0.05$): (———) theory; (+, ×) final estimates; and (— — —) 'best fit' ellipse.

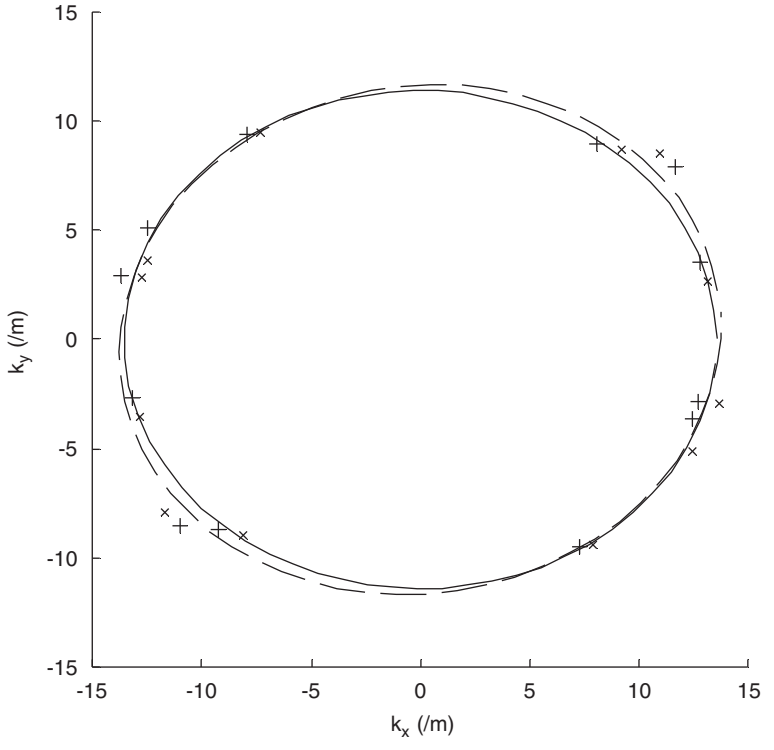

Fig. 17. Wavenumber estimates in non-resonant plate simulation (12-wave model, $\eta = 0.05$): (———) theory; (+, ×) final estimates; and (— — —) 'best fit' ellipse.

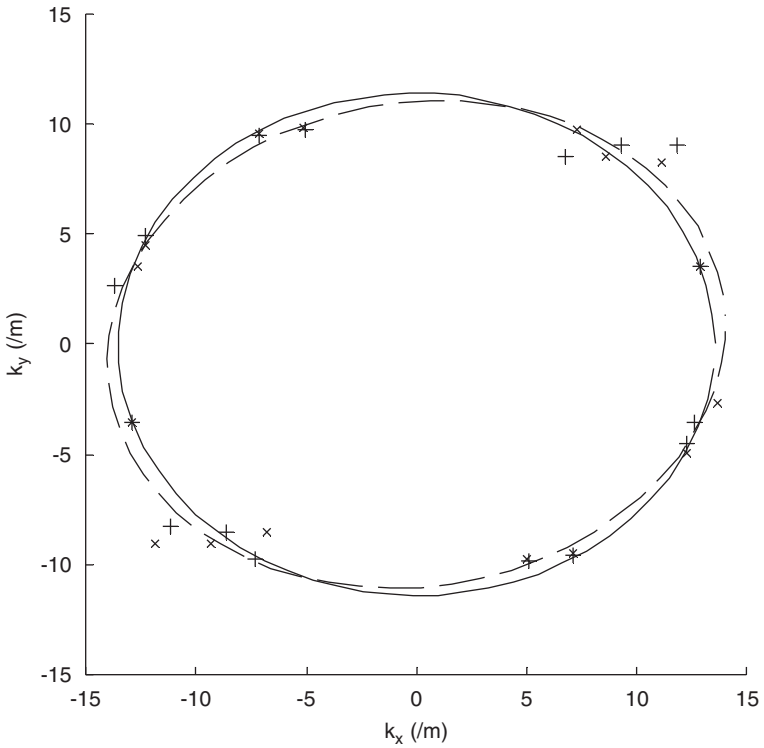

Fig. 18. Wavenumber estimates in non-resonant plate simulation (16-wave model, $\eta = 0.05$): (———) theory; (+, ×) final estimates; and (— — —) 'best fit' ellipse.

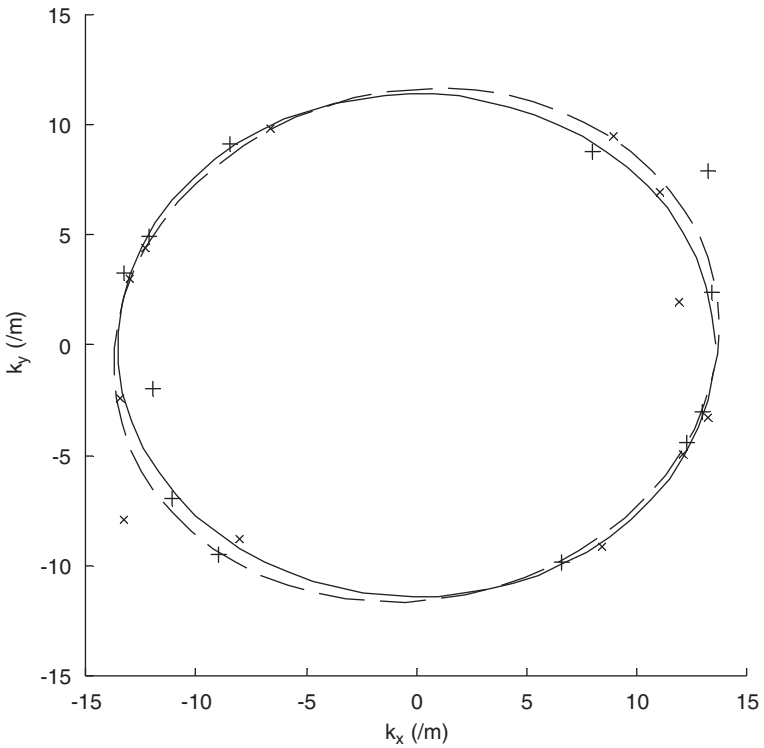

Fig. 19. Wavenumber estimates in non-resonant plate simulation (12-wave model, $\eta = 0.05$, SNR = 20 dB): (———) theory; (+, ×) final estimates; and (— — —) 'best fit' ellipse.

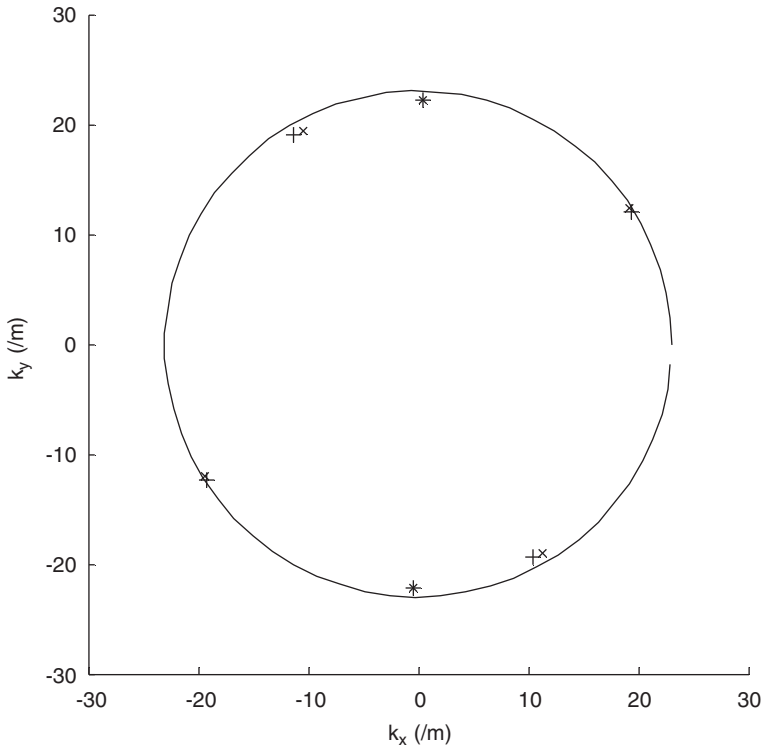

Fig. 20. Wavenumber estimates in non-resonant steel plate (six-wave model): (———) theory and (× , +) final estimates.

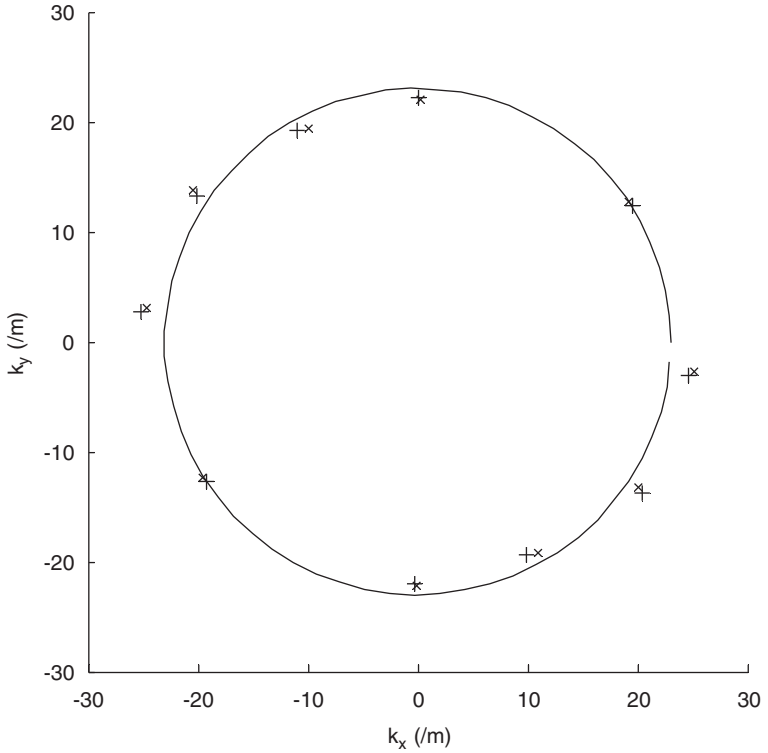

Fig. 21. Wavenumber estimates in non-resonant steel plate (10-wave model): (———) theory and (× , +) final estimates.

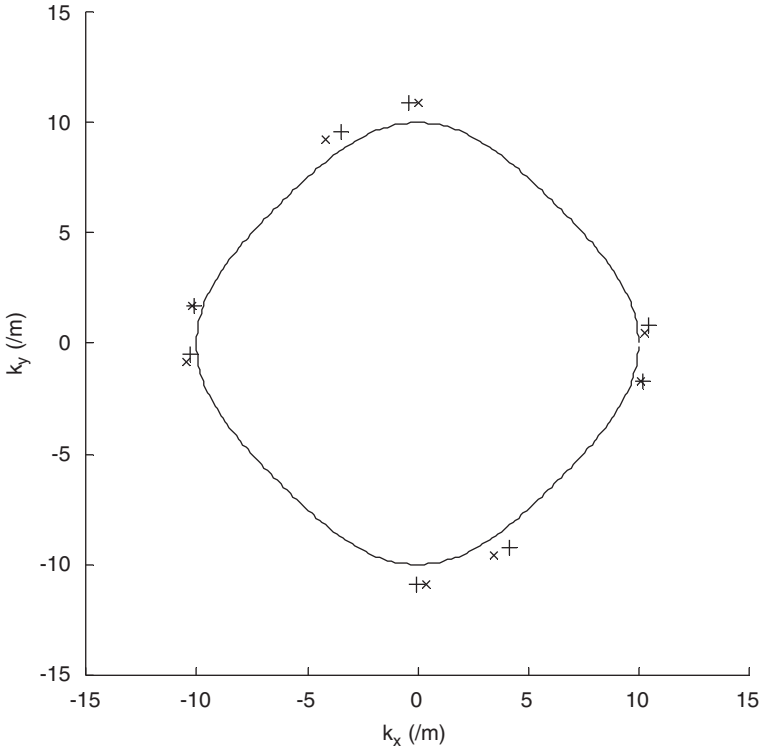

Fig. 22. Wavenumber estimates in non-resonant composite plate (eight-wave model): (———) theory and (× , +) final estimates.

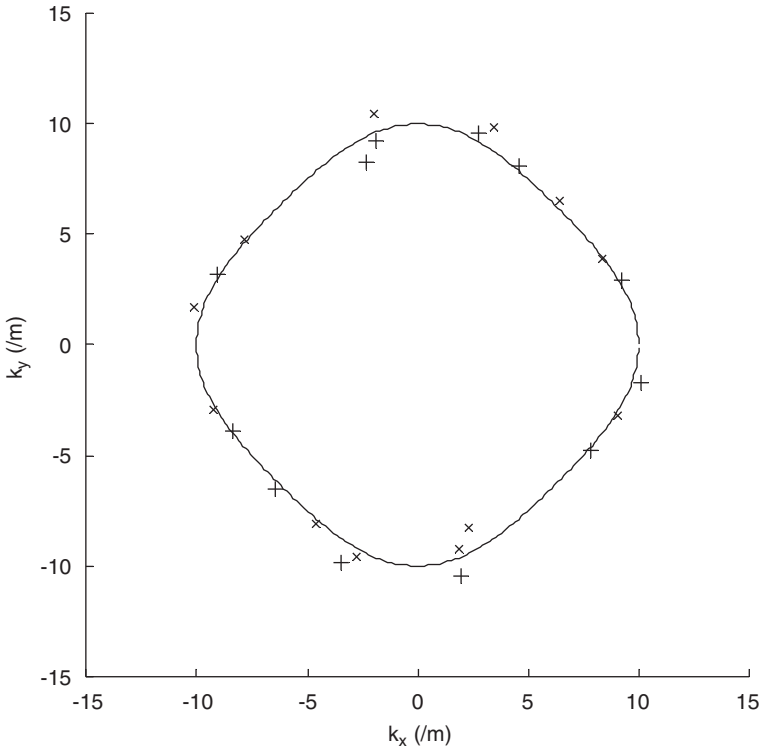

Fig. 23. Wavenumber estimates in non-resonant composite plate (12-wave model): (———) theory and (× , +) final estimates.

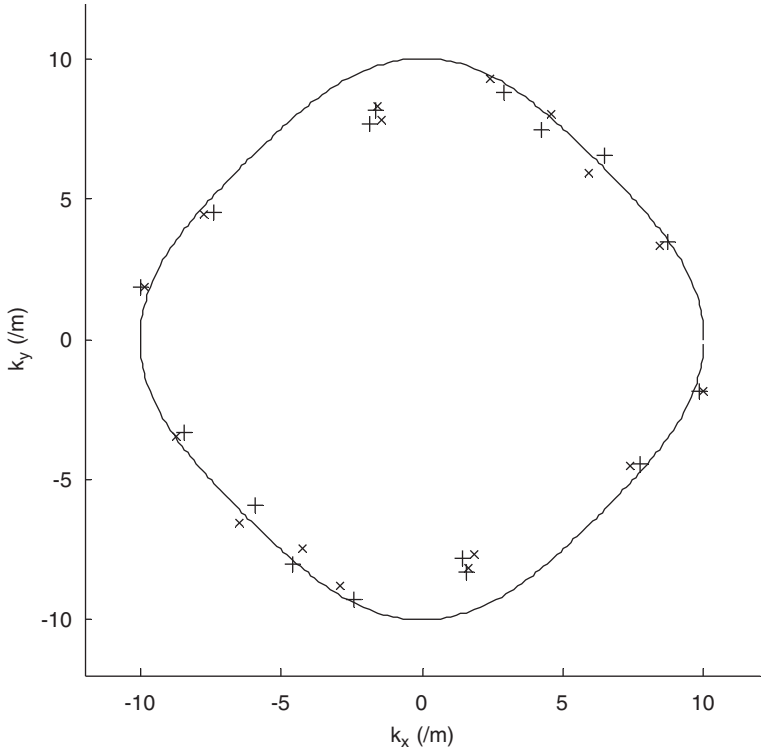

Fig. 24. Wavenumber estimates in non-resonant composite plate (16-wave model): (———) theory and (× , +) final estimates.

analysis. Confidence in the results comes from observed convergence to a solution that seems physically reasonable.

Acknowledgements

The author gratefully acknowledges the assistance of ISVR, Southampton, UK, and KTH, Stockholm, Sweden, in this work. The work had its roots in the author's sabbatical leave at ISVR, where the experimental measurements were also performed. The theoretical work and simulations were undertaken while on sabbatical leave at KTH.

References

[1] K. Grosh, E.G. Williams, Complex wave-number decomposition of structural vibrations, *Journal of the Acoustical Society of America* 93 (2) (1993) 836–848.

[2] P.J. Halliday, K. Grosh, Maximum likelihood estimation of structural wave components from noisy data, *Journal of the Acoustical Society of America* 111 (4) (2002) 1710–1717.

[3] J.S. Bolton, H.J. Song, Y.K. Kim, The wavenumber decomposition approach to the analysis of tire vibration, *Proceedings of NoiseCon 98,* Ypsilanti, Michigan, USA, April 1998, pp. 97–102.

[4] J.S. Bolton, Y.-J. Kim, Wave number domain representation of tire vibration, *Proceedings of Internoise 2000*, Nice, France, August 2000.

[5] A.J. Hull, D.A. Hurdis, An inverse method to measure the flexural wave properties of a beam, *Materials Science Forum* 440–441 (2003) 329–336.

[6] J.G. McDaniel, W.S. Shepard Jr., Estimation of structural wavenumbers from spatially sparse response measurements, *Journal of the Acoustical Society of America* 108 (4) (2000) 1674–1682.

[7] N.S. Ferguson, C.R. Halkyard, B.R. Mace, K.H. Heron, The estimation of wavenumbers in two-dimensional structures, *Proceedings of the ISMA International Conference on Sound and Vibration*, vol. 2, Leuven, Belgium, September 2002, pp. 799–806.

[8] J. Berthault, M.N. Ichchou, L. Jezequel, K-space identification of apparent structural behaviour, *Journal of Sound and Vibration* 280 (2005) 1125–1131.

[9] R. de Prony, Essai experimental et analytique, *Journal de l'Ecole Polytechnique* 1 (1795) 24–76.
[10] V.F. Pisarenko, The retrieval of harmonics by linear prediction, *Geophysics Journal of the Royal Astronomical Society* 33 (1973) 347–366.
[11] M.R. Osborne, Some special non-linear least squares problems, *SIAM Journal of Numerical Analysis* 12 (1975) 571–592.
[12] R.J. Unglenieks, R.J. Bernhard, Measurement of flexural structural intensity using wavenumber techniques, *Proceedings of the Fourth International Congress on Intensity Techniques*, Senlis, France, 31 August–2 September 1993, pp. 305–311.
[13] G.H. Golub, V. Pereyra, The differentiation of pseudo-inverses and non-linear least squares problems whose variables separate, *SIAM Journal of Numerical Analysis* 10 (1973) 413–432.
[14] P. Eykhoff, *System Identification: Parameter and State Estimation*, Wiley, London, 1974.
[15] G.K. Smyth, D.M. Hawkins, Robust frequency estimation using elemental sets, *Journal of Computational and Graphical Statistics* 9 (2000) 196–214.
[16] A.W. Leissa, *Vibration of Plates. SP160 NASA*, US Government Printing Office, Washington, DC, USA, 1969.
[17] K.H. Heron, Predictive SEA and anisotropic panels, *Proceedings of the ISMA International Conference on Sound and Vibration*, Leuven, Belgium, September 2002.